Direct-Contact Steam Condensation with Simultaneous Noncondensable Gas Absorption

Vasilis Bontozoglou and Anastasios J. Karabelas
Chemical Process Engineering Research Inst. and Dept. of Chemical Engineering,
Aristotle University of Thessaloniki, GR 54006 Thessaloniki, Greece

Experimental results are reported on simultaneous heat transfer and gas dissolution during the direct-contact condensation of steam on water in the presence of CO_2. A column filled with structured packing is used as condenser with the water in counterflow with the steam/CO_2 mixture. The region along the column where the bulk of condensation takes place is controllable by suitable choice of the steam/water ratio. Measured local heat-transfer coefficients change by roughly an order of magnitude from the bottom to the top of the column. The extent of CO_2 dissolution in the water/condensate under most conditions is unexpectedly high and depends strongly on the exit liquid temperature. A driving force based on the interfacial CO_2 concentration, not the overall concentration difference used in conventional absorption operations, is suggested as more appropriate to describe the phenomenon. The data are complemented with preliminary results from a computational model based on the integration along the column of local heat- and mass-transfer rates.

Introduction

Direct-contact heat transfer is already diversely applied throughout the process and related industries; for example in physical separations, water desalination, and steam condensation in power plants. The use of direct-contact vs. surface transfer offers some distinct advantages. First, the exchange surfaces represent a major expense of the total system and are subject to corrosion and fouling. Furthermore, using a solid surface to transfer heat between two fluids requires a significant temperature difference, which results in loss of overall system efficiency. As the cost of energy grows, direct-contact devices are being given new consideration, since they offer the possibility of improved performance with reduced capital expenses (Kreith and Boehm, 1988).

Lack of reliable design techniques of general applicability, like the ones available for conventional configurations, delays the development of direct contact processes. Indeed, direct-contact devices are typically viewed as special situations, and empirical design procedures are often developed without the underpinnings of a basic physical understanding of related phenomena (Kreith and Boehm, 1988).

This article discusses direct-contact condensation of steam on water in the presence of noncondensable gases. This particular combination is encountered in various applications such as power-plant condensers, ocean thermal energy conversion systems, and geothermal installations. It is also relevant to the nuclear industry in certain safety evaluation scenarios (Tung and Dhir, 1988).

The application motivating this study is the separation of noncondensable gases from high pressure geothermal steam upstream of the turbines. "Upstream removal" protects turbine components from corrosion, leads to higher conversion efficiency, and permits more effective H_2S pollution abatement. A type of process which has been proposed as suitable for this task (Coury, 1985; Awerbuch et al., 1985) involves condensation of steam at high pressure, where the bulk of noncondensables escapes with the gas stream. Subsequent flashing of the condensate produces clean steam and a cooler liquid for recycle to the condenser. For this design to work, however, it is essential to minimize the amount of noncondensables dissolved in the liquid. Preliminary calculations have indicated that countercurrent flow of steam and water leads to less gas absorbed. Therefore, a design involving a column filled with structured packing was selected.

Current address of V. Bontozoglou: Dept. of Mechanical Engineering, University of Thessaly, GR-38334 Volos, Greece.

Literature in the area of direct-contact condensation is limited. Fair (1972) summarizes available correlations for gas and liquid side heat-transfer coefficients for various types of contactors including beds with random packing. His design methods, however, are limited to conditions where the sensible and latent heat loads are of comparable magnitude. Very few data are included for conditions where the latent load is the major heat duty of the contactor.

Sideman and Moalem-Maron (1982) provide a thorough review of relevant studies until about 1980. Wilke et al. (1963), Harriott and Wiegandt (1964), and Jacobs et al. (1979) report data on the condensation of pure vapors on different liquids using columns filled with various random packings. In all these works, the major resistance to condensation resides in the liquid. An extensive study of various condenser configurations for steam condensation on water in the presence of noncondensable gases was undertaken by Bharathan and Althof (1984). Data are reported for commercial cooling-tower fills and low temperatures and pressures, relevant to open-cycle ocean thermal energy conversion systems.

Two phenomena are given major consideration in this article. First, the heat-transfer rate is studied and related coefficients are reported. The new data complement the aforementioned studies of condensation in packed beds with random packings and commercial cooling-tower fills. Secondly, the extent of gas absorption in the liquid is measured. These results test the suitability of the proposed device for the particular geothermal task. They also allow us to study the condensation process in the presence of *noncondensable, but slightly soluble*, gases. Common gas dissolution has been mostly neglected in heat-transfer models (Jacobs, 1988).

The experimental data are complemented with preliminary results from a computational model, based on the integration along the column of local heat- and mass-transfer rates. The simulation provides valuable insights into the relative significance of various resistances to mass and heat transfer along the column, thus facilitating the interpretation of experimental results. At its present state of development, however, the simulation algorithm is not fully predictive.

In the next section, the apparatus built and the experimental procedure followed during data collection are described. Then, the computational procedure and relevant correlations are presented. In the subsequent section, results pertaining to heat- and mass-transfer rates along the column are discussed. Finally, some concluding remarks are offered.

Experimental Apparatus and Procedure

The experimental system is shown in Figure 1. Tap water is demineralized and delivered to a spray manifold at the top of the column. The water flow rate is controlled by a PID controller (Shimaden, SR-24) and a flowmeter (Signet, Rotor XLF), which electronically actuate a 1/2 in. Badger valve. Steam is provided by a central generator and is fed to the bottom of the column after going through a condensate separator and a pressure reducer. CO_2 is delivered to the steam line from supply cylinders, and its flow rate is measured with rotameters and adjusted by precision valves.

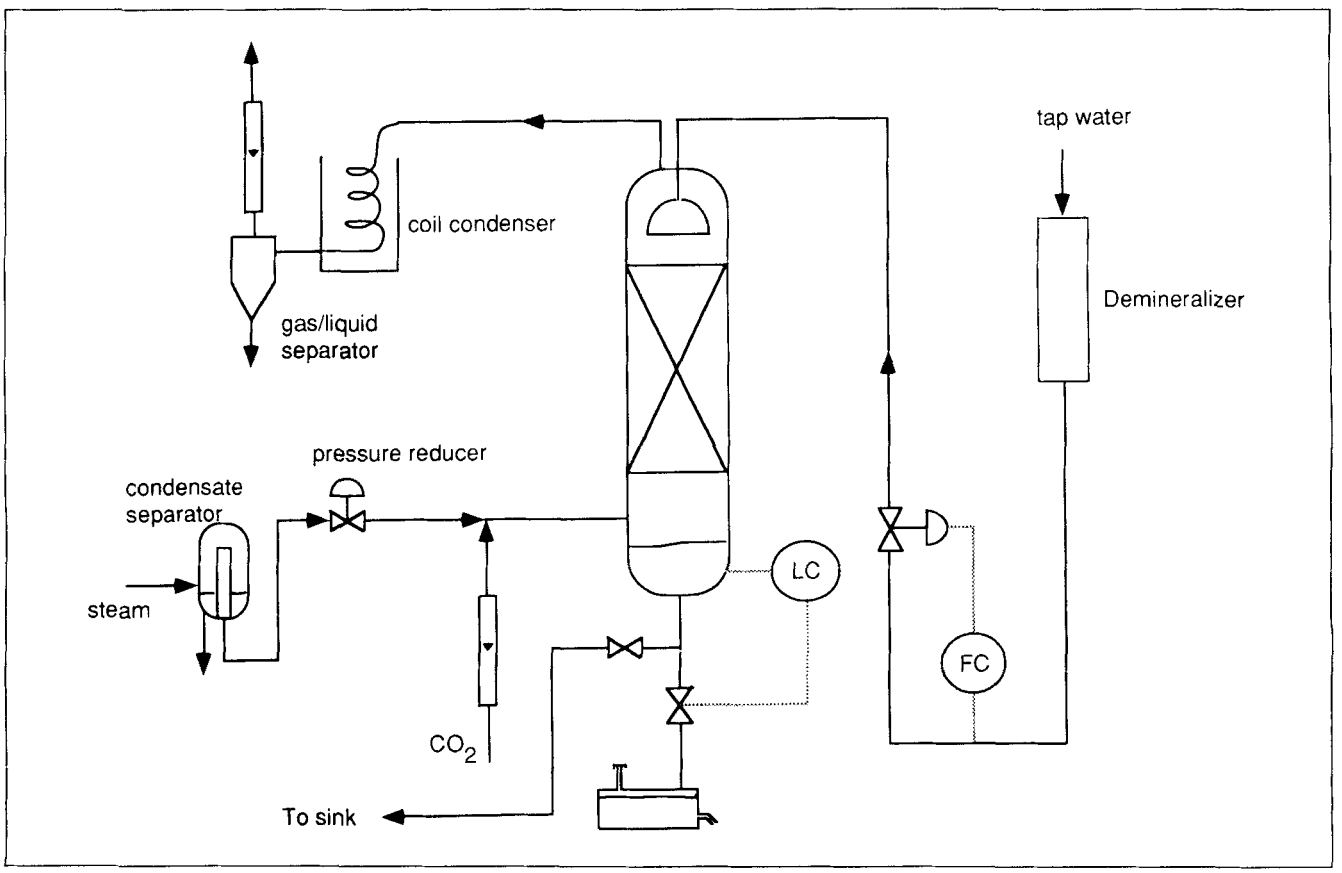

Figure 1. Experimental setup.

A stainless steel tank with a volume of 25 L is provided at the bottom exit of the column. Through a system of automatically operated pneumatic valves, the effluent liquid stream can be directed to the tank and the time required to fill it is recorded. This serves as an indirect method of determining the steam flow rate (= total liquid outflow − cold water inflow).

The vapor stream exiting from the top of the column passes through a coil condenser so that the steam vent condenses and separates from the noncondensable gas. The remaining gas (CO_2 saturated at ~20°C) passes through a rotameter and is then released to the atmosphere.

The condenser is a 1.05-m-long, 0.15-m-ID column made of stainless steel. The column consists of a maximum of three sections (0.1, 0.2 and 0.4 m long), which can be combined to provide a useful length ranging from 0.1 to 0.7 m. A hot well, equipped with a magnetic floater, forms the bottom of the column. The liquid outlet valves are electrically actuated through this floater in order to prevent the passage of vapor in the drainage pipe. The entire condenser is wrapped with a thick layer of glass wool to provide insulation.

The column is filled with Mellapak 250.Y structured packing marketed by Sultzer. More details about packing dimensions are provided in the next section. Interest in structured packing stems from its favorable performance characteristics (Fair and Bravo, 1990). In particular, low pressure drop is highly desirable in the reboiling of geothermal steam, because any reduction in pressure carries with it a severe energy penalty. It is also noted that condensation data do not seem to be available for this kind of packing.

Temperatures are monitored with K-type thermocouples calibrated to ±0.2°C. The thermocouples are located at the water inlet, the water-condensate outlet, and the vapor inlet lines. Four more thermocouples are embedded in the packing at about 4 cm intervals, starting from the lower bed support. Their tips are positioned close to the center of the column cross section in contact with the packing to provide the temperature of the local liquid film. All temperature measurements are indicated on a central panel and are also recorded by a data acquisition system (AI13 interface on an Apple IIe) for later processing.

Pressure measurements are taken at various locations along the flow. Pressure indicators are installed on the steam/condensate separator, the steam line before the entrance in the hot well and the vapor exit line at the top of the column. A mercury manometer is connected to the hot well and measures the pressure difference with the ambient. Its indication is used to determine the liquid-vapor saturation point. Finally, manometers are installed to measure pressure drop along the packing.

Determination of the amount of CO_2 dissolved in the liquid involves the following procedure. The indications of the entrance and exit CO_2 rotameters are recorded, after the entrance value is corrected by taking into account the pressure at the point where the CO_2 tube joins the steam line. The difference between the two values is the amount of CO_2 dissolved in the water. This amount is also measured directly by the following procedure which is more accurate. A sample of liquid is drawn from the hot well using a 10-mL syringe. The syringe contains a small quantity of dilute NaOH solution with phenolphthalein indicator to ensure that the CO_2 dissolved in the condensate is trapped. The amount of liquid withdrawn is such that the indicator does not turn colorless, which guarantees that the CO_2 is in the form of HCO_3^- and CO_3^{2-}. Determination of the total amount of CO_2 is accomplished by titration with HCl solution, that is, recording the amount of acid needed to bring the liquid from pH = 9 (phenolphthalein indicator) to pH = 4.2 (methyl red indicator). A similar determination is done for the inlet water, and the difference provides the amount of CO_2 absorbed during condensation.

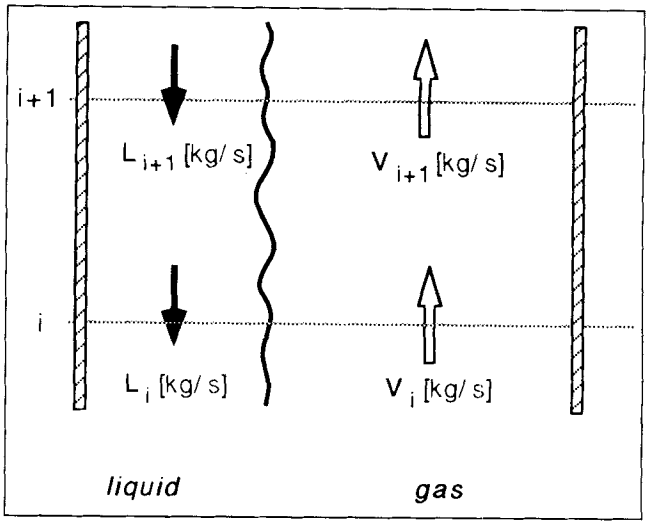

Figure 2. Typical section in the numerical model of the column.

Computational Procedure

Numerical scheme

An important feature of the direct-contact process presently studied is the very drastic change of flow rate and composition of the vapor phase along the column. These changes affect the driving force for condensation as well as the transfer coefficients. As a result, design procedures for direct-contact condensers are mostly empirical (Kreith and Boehm, 1988). One challenge of the computational scheme lies in accurately describing this rapid evolution.

The approach presently tested is based on the numerical integration of local transfer rates. Mass-transfer coefficients from correlations developed for gas/liquid absorption are used, and heat-transfer coefficients are estimated by analogy arguments. The column is split into a number of sections, each one effecting the condensation of a fixed percentage of inlet steam (Figure 2). The liquid and gas flow rates and the gas-phase composition at each cross section are directly calculated by mass balances. If DV_i is the mass rate of steam condensing in section $(i, i + 1)$ then:

$$V_{i+1} = V_i - DV_i \tag{1}$$

The noncondensable gas is assumed to remain in the gas phase. Therefore, if G is its mass-flow rate at the entrance, the mole fraction of steam at the cross section i is:

$$y_{st,i} = \frac{V_i/M}{V_i/M + G/M'} \tag{2}$$

where M and M' are the molecular weights of water and gas. From the gas-phase composition, its bulk temperature is calculated using the assumptions that the gas is saturated in steam and that the change in pressure along the column is negligible. Then, the liquid temperature at the section boundaries is determined from an energy balance of the form:

$$V_i H_{st,i} + GH_{nc,i} + L_{i+1}H_{l,i+1} = V_{i+1}H_{st,i+1} + GH_{nc,i+1} + L_{i+1}H_{l,i} \quad (3)$$

Finally, the height of each column section is computed as:

$$\Delta z_i = \frac{Q_i}{U_{i/i+1}\, A_{i/i+1}\, \Delta T_{i/i+1}} \quad (4)$$

where $U_{i/i+1}$, $A_{i/i+1}$, $\Delta T_{i/i+1}$ are the arithmetic mean between i and $i+1$ of the local overall coefficient, interfacial area, and gas/liquid temperature difference. In particular, the local transfer coefficients are computed from correlations appropriate for structured packing using transport properties evaluated at the bulk temperature of the cross section. In this way, it is anticipated that the wide temperature variations along the column are correctly accounted for.

In the calculation of a local overall heat-transfer coefficient, U, the combined resistance due to sensible heat convection and steam diffusion through the inert gas is considered and the following expression is obtained:

$$h_g(T_g - T_i) + k_g H_v(p_g - p_i) = h_l(T_i - T_l) = U(T_g - T_l) \quad (5)$$

Interfacial resistance is ignored, as it is known to be insignificant for the steam/water system (Sparrow et al., 1967). The mass-transfer coefficient, k_g, for diffusion through a stagnant gas layer is used and the vapor-phase coefficient, h_g, is modified by an Ackermann-type correction (Wang and Tu, 1988) to account for the effect of mass transfer on heat transfer.

For comparison with the experimentally measured volumetric heat-transfer coefficient, the computed local overall coefficient, U, must be multiplied with the specific area available for heat transfer. This is taken to be the nominal area of the packing. The alternative of using a correlation of wetted fraction developed for absorption columns was not preferred, as steam condensation is expected to wet the packing rather thoroughly.

At its present state of development, the simulation neglects the effect of liquid free-fall space below the packing. This effect is generally expected to be significant both for steam condensation and gas absorption. It does become insignificant for condensation only under certain experimental conditions, as explained later. Thus, quantitative comparisons between predictions and experimental data are presented only for heat transfer and for the specific conditions.

Reservations may be expressed about the validity of the above approach. The use of mass-transfer data for condensation calculations has been criticized as not always safe (Jacobs et al., 1979). An additional question remains relative to the fact that correlations in the literature are usually developed from experiments with constant vapor and liquid flow rates. Therefore, the presently proposed numerical procedure tacitly assumes a pseudo steady-state operation, whereby conditions relax faster than the change in vapor flow rate. Despite these words of caution, the numerical results demonstrate an encouraging agreement with condensation data, and the procedure seems to deserve further consideration.

Concerning the absorption rate of CO_2 in the liquid, it is posited that the rate of dissolution is too small to affect the condensation process. Therefore, condensation is modeled by considering the interface as impermeable to the gas, and the absorption computation is undertaken at the end using the vapor CO_2 concentrations resulting from the condensation calculation.

This approach represents a first approximation and further refinement is evidently needed. Even at this level of sophistication, there is some uncertainty concerning the correct driving force to be used for CO_2 absorption, as the rapid condensation of steam is expected to result in high noncondensable gas concentration in the vapor region close to the interface. This point is clarified in the next section by a comparative assessment of the experimental data with numerical predictions. Detailed comparison between computational and experimental results is not possible, as previously mentioned. Nevertheless, there is order of magnitude agreement, which indicates that the notion that CO_2 absorption is governed by interfacial rather than bulk concentration is in the correct direction.

Table 1. Characteristics of Structured Packing

Specific Area (m^{-1})	250
Void Fraction	0.95
Corrugation Angle	45°
Crimp Height (m), h	0.0119
Corrugation Side (m), s	0.0171
Corrugation Base (m), b	0.0241

Parameters used

The main dimensions of Mellapak 250.Y (the packing used in this work) are shown in Table 1. The packing consists of closely spaced corrugated sheets with gas flow channels at an angle 45° to the horizontal. Liquid spreads over the treated surface and flows downward. It can, therefore, be approximated by a laminar film flowing down a short vertical plate (Haan and Graauw, 1991). The present computations are based on a mass-transfer model developed for various structured packings by Fair and Bravo (1990). Correlations for the vapor and liquid phase are expressed in terms of *Sh* and *Re* numbers, using an equivalent diameter and suitably defined effective liquid and vapor velocities.

Following Haan and Graauw (1991), the average available perimeter per unit cross section is:

$$P = \frac{4s + b}{bh} \quad (6)$$

where s, b and h are the characteristic dimensions of the packing given in Table 1. Based on Eq. 6, an equivalent diameter, d_{eq}, is defined as:

$$d_{eq} = \frac{4}{P} = \frac{4bh}{4s + b} \quad (7)$$

The effective vapor velocity through the channels is related to the superficial velocity by the equation:

$$u_{v,\text{eff}} = \frac{u_{vs}}{\epsilon \sin \theta} \tag{8}$$

where it is assumed that the liquid film thickness is too small to affect the void fraction.

The effective liquid velocity is approximated by the surface velocity of a laminar film (with the local flow rate), flowing down a vertical wall:

$$u_{l,\text{eff}} = \frac{3\Gamma}{2\rho_l}\left[\frac{\rho_l(\rho_l - \rho_v)g}{3\mu_l\Gamma}\right]^{1/3} \tag{9}$$

where $\Gamma = L/\text{PA}_t$, L is the mass-flow rate, and PA_t the total wetted perimeter at every cross section. It is noted once more that, in our case, both $u_{l,\text{eff}}$ and $u_{v,\text{eff}}$ change along the column. Following Fair and Bravo (1990), the vapor-phase mass-transfer coefficient is estimated from the relation for wetted-wall columns:

$$Sh = 0.034\ Re^{0.8}\ Sc^{0.33} \tag{10}$$

where $Sh = k_v d_{eq}/D_v$, $Re = \rho_v(u_{l,\text{eff}} + u_{v,\text{eff}})/\mu_v$ and $Sc = \mu_v/\rho_v D_v$. The coefficient k_v is corrected for diffusion of steam through a stagnant gas film and is expressed in terms of a pressure driving force.

For the liquid phase, a penetration model is used with the exposure time taken as the residence time for vertical liquid flow between corrugation changes. The result is:

$$k_l = 2\sqrt{D_l/\pi t} = 2\left(\frac{D_l u_{l,\text{eff}} \cos\theta}{\pi s}\right)^{1/2} \tag{11}$$

Heat-transfer coefficients h_g and h_l are estimated from the Chilton-Colburn analogy (Treybal, 1980). Finally, the vapor-phase coefficient is modified by the following Ackermann-type correction (Wang and Tu, 1988) to account for the effect of mass transfer on heat transfer:

$$h_g' = \frac{N_{st}M_{st}C_{p\cdot st}}{1 - \exp(-N_{st}M_{st}C_{p\cdot st}/h_g)} \tag{12}$$

Results and Discussion

The critical parameters varied in these experiments are the mass-flow rates of water, steam, and CO_2. The height of the packing is kept constant and equal to 72 cm and the steam vent rate from the top of the column may or may not be equal to zero. Temperatures at intermediate locations along the column are used to determine local heat-transfer coefficients, which are essentially average coefficients for the respective small segment of packing.

A preliminary observation during the condensation process is that most of the column height remains inactive. With a packing 72 cm high and typical condensation lengths less than 20 cm, this should come as no surprise. What is most interesting, however, is that the region along the column where the bulk of condensation occurs is subject to control by suitable choice of the steam-to-water ratio. This is demonstrated in Figure 3, which shows the variation of water temperature upward from the hot well when decreasing the water flow rate or increasing the steam load. In particular, the following observations are made. For small steam rates, there is a considerable change in the liquid temperature from the end of the packing to the hot well. This indicates that significant condensation takes place in the free-fall space at the bottom of the packing and the measured rates may reflect the performance characteristics of this region rather than that of the packing itself.

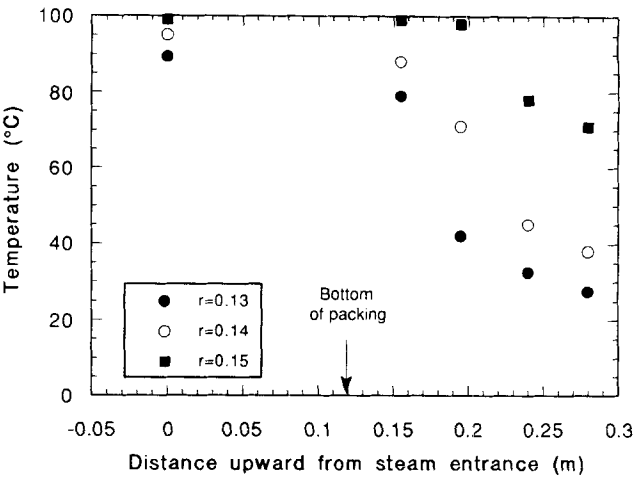

Figure 3. Liquid temperatures in the column, upstream from the hot well, for various inlet steam/water ratios, *r*.

As the steam flow rate increases for constant water rate, the reading of the first thermocouple (embedded 3.5 cm from the bottom of the packing) approaches that of the hot well, indicating that the reduction in vapor loading at the bottom of the column becomes insignificant. Further increase in the steam flow rate moves the region of drastic change of the liquid temperature towards the upper part of the bed. Finally, when the steam supply is increased to the point that complete condensation is not possible, the liquid along most of the column length is practically at the saturation temperature, and condensation takes place in the free space below the water spray manifold and in the first few centimeters of packing.

The aforementioned phenomenon is of profound significance here. For one, it provides a means of rendering negligible the effect of the free-fall space below the packing (at least as far as condensation is concerned), thus facilitating comparisons with computer results. Even more importantly, it is shown to have a dominant influence on the percent of CO_2 dissolved in the liquid, thus controlling the extent of gas separation.

Heat-transfer results

Temperature measurements of the liquid phase are taken at the inlet and outlet of the column and at four points close to the bottom of the packing. The exit temperatures, together with the steam and water flow rates, are used to check the heat balance closure. Differences are consistently less than 10%.

Temperatures at intermediate points are used to calculate the volumetric heat-transfer coefficient for each section between consecutive measuring locations. These measurements are considered to provide only a crude approximation of local values.

To process the data, the following assumptions are made:

- The sensible heat changes of steam and inert gas are considered small compared to the latent heat of condensation and are ignored in the calculation.
- The liquid flow rate is taken as constant within each section (cooling water + previously accumulated condensate).
- The bulk temperature in the gas phase is the saturation temperature of steam. However, because of the small initial concentration of inerts and the location of the measuring points close to the bottom of the column, this calculated temperature differs less than 2% from the entrance gas temperature, T_g.

Data treatment proceeds as follows. From the measured values T_{l1} and T_{l2}, the heat load of each section is calculated as:

$$Q = m_l C_{p,l} (T_{l1} - T_{l2}) = \Delta m_{st} H_v \tag{13}$$

From the steam condensation rate inside the section, Δm_{st}, the new steam content of the gas phase and the respective saturation temperatures, T_{g1} and T_{g2}, are calculated. Then, the local volumetric coefficient is computed as:

$$U_v = \frac{Q}{A_t \Delta z (\Delta T)_{\ln}} \tag{14}$$

where A_t is the column cross-sectional area, Δz is the section height, and $\Delta T_{\ln}$ is the log mean temperature difference.

Data refer to two different modes of operation, corresponding to water effectiveness, ϵ_w, less than one or roughly equal to one. The water effectiveness is defined as $\epsilon_w = (t_{l,\text{out}} - t_{l,\text{in}})/(t_{g,\text{in}} - t_{l,\text{in}})$ and provides a measure of the water temperature rise as it relates to the overall available temperature difference (subscripts in and out stand for inlet and outlet).

When operating the condenser with a steam load approaching the maximum water effectiveness ($\epsilon_w \approx 1$), the liquid temperature at the hot well does not differ significantly from the one recorded at the bottom of the packing. The data in Figure 3, corresponding to steam/water ratio $r = 0.15$, are typical of such temperature distributions. Data taken under these conditions correspond to condensation taking place exclusively within the packing volume and are suitable for direct comparison with the numerical predictions. Figure 4 is a comparison of four different flow rates and steam loads, all with 3% w/w CO_2 in the entrance steam and water effectiveness very close to one. Points represent measurements and lines are results of the numerical simulation. The observed satisfactory overall agreement indicates that the simulation algorithm is in general capable of describing the drastic changes occurring as condensation proceeds along the column.

In particular, both experiment and computation demonstrate a rather sharp decrease of heat-transfer rate along the packing. A systematic analysis of the significance of the various resistances can be performed for the computer simulation, and the results in terms of partial and overall transfer coefficients are demonstrated in Figure 5. An inspection indicates that the

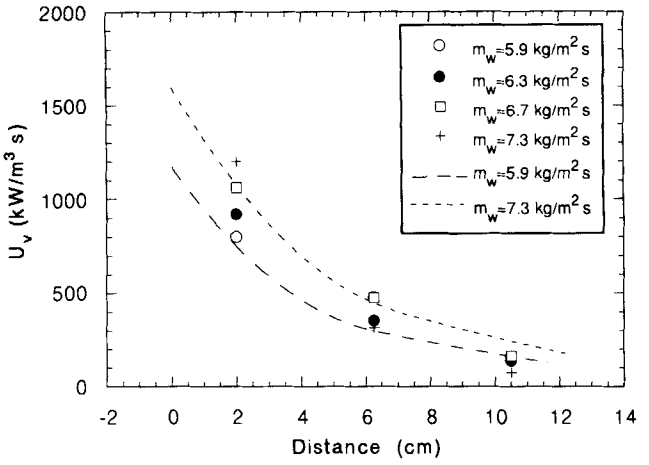

Figure 4. Local heat-transfer coefficients at different locations along the packing for constant steam/water ratio, r = 0.15.

decrease in overall heat-transfer rate may be caused by a parallel reduction of the mass-transfer coefficient for steam diffusion in the vapor phase. The decrease of the mass-transfer coefficient is attributed to the following two factors. First, the well-known effect of inerts during steam condensation is of significance. Inert gas buildup at the vapor/liquid interface leads to a lower partial pressure of the steam, which in turn lowers the interface temperature at which condensation occurs and correspondingly decreases the thermal driving force. This phenomenon has been shown (Sparrow et al., 1967) to depend directly on the mass fraction of noncondensables. Therefore, as the steam progressively condenses along the column, the concentration of CO_2 in the remaining gas phase continuously increases, leading to significantly lower heat-transfer rates. Another factor is related to the gas Reynolds number which decreases continuously along the column, leading to an almost proportional ($Sh \approx Re^{0.8}$) reduction of the partial mass-transfer coefficient in the gas phase. The partial heat-transfer coeffi-

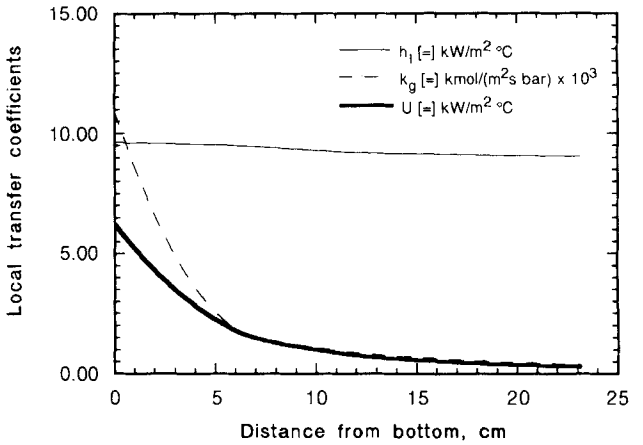

Figure 5. Variation of heat- and mass-transfer coefficients along the column.

Terms h_l, k_g, and U are respectively the partial heat-transfer coefficient in the liquid, partial mass-transfer coefficient in the gas, and overall heat-transfer coefficient.

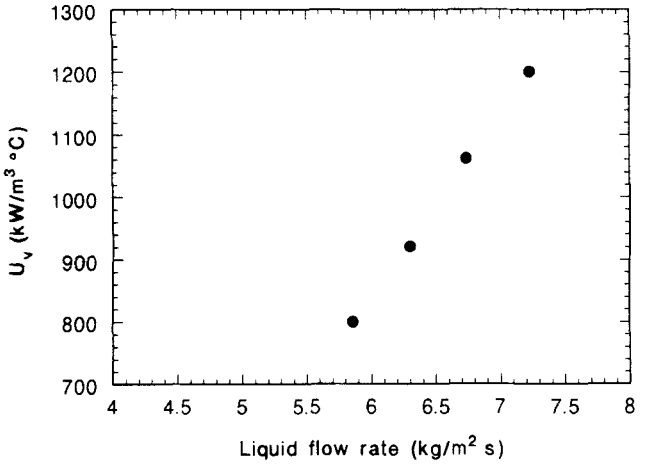

Figure 6. Heat-transfer coefficients at approximately 2 cm above the base of the packing as a function of liquid flow rate for constant steam/water ratio r = 0.15.

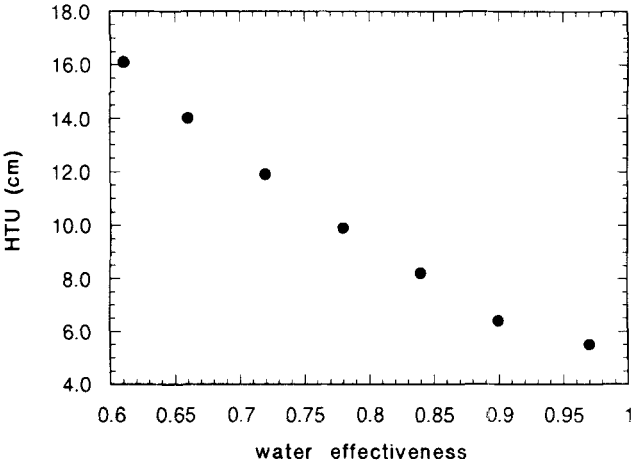

Figure 8. Height of a transfer unit as a function of the water effectiveness, ϵ_w.

cient follows the same trend, but the contribution of sensible heat transfer is evidently negligible compared to the latent heat transfer which is influenced by the mass-transfer coefficient.

In an experimental study of direct-contact steam condensation on falling water films (Karapantsios et al., 1992) in the presence of large amounts of noncondensables it was observed that by increasing the liquid flow rate smaller values of integral heat-transfer coefficients were obtained. It is also noted here (Figure 4) that with increasing distance from the bottom of the column, corresponding to an increasing fraction of noncondensables, the higher liquid flow rates appear to be associated with smaller values of the heat-transfer coefficients. Whether this is a systematic trend enhanced by increasing amounts of noncondensables remains to be examined.

The range of liquid- and gas-flow rates covered in the present series of experiments is such that the hydrodynamic loading at the bottom of the column is around 40 to 60% of flooding. Given that the bottom is the location with the highest loading,

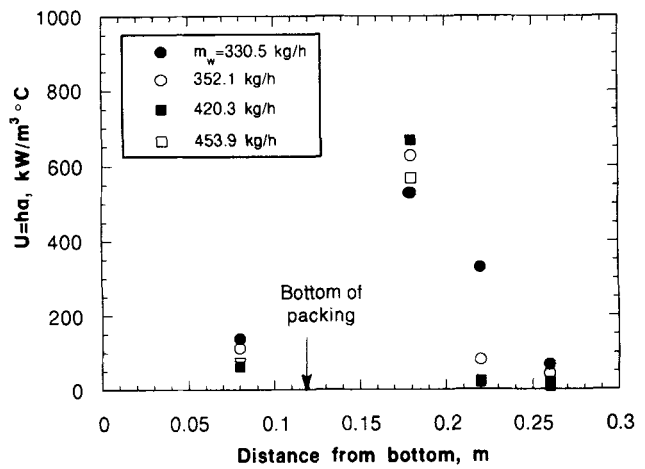

Figure 7. Local heat-transfer coefficients under partial condensation conditions at the hot well below the packing.

what is interesting is the effect of the approach to flooding on the local heat-transfer coefficient. Figure 6 shows such results for the first 4-cm-thick section of packing, and the liquid flow rates and steam loads of Figure 4. Figure 6 shows that there is an almost linear dependence of the heat-transfer coefficient on the liquid flow rate. This, however, is a preliminary conclusion and experiments closer to flooding are needed to check its validity.

When the water flow rate is in excess for a given steam load, the liquid exit temperature is less than the steam entrance temperature ($\epsilon_w < 1$). Under these conditions, part of the condensation takes place at the free-fall space below the packing. However, probably because of the poor liquid distribution in this region, the local heat-transfer coefficient measured is relatively low, rising to a maximum in the first centimeters of packing. This behavior is demonstrated in Figure 7.

Overall volumetric heat-transfer coefficients may be expressed in terms of the height of a transfer unit (HTU). Plotted in Figure 8 is the variation in HTU with the water effectiveness factor, ϵ_w, considering as an integral section the lower 16 cm of packing. It is observed that the HTU decreases with increasing ϵ_w (being almost inversely proportional to ϵ_w for ϵ_w values less than one) and approaches a minimum value for ϵ_w close to 1. These observations are in agreement with similar findings of Bharathan and Althof (1984), except that the minimum value presently found is around 5 cm, whereas their value for the packed bed is 27 cm. The difference may be attributed to the lower ambient pressure in their experiments and, to some extent, to the superior performance characteristics of structured packings.

Mass-transfer results

In the experiments reported with $\epsilon_w < 1$, condensation takes place in the lower part of the packing and the undissolved CO_2 stream flows upward, countercurrently with the free falling water stream. It is found that, with this setup, there is enough contact area for the cold water to get saturated in CO_2 at the upper part of the packing. It is expected that this concentration is higher than any other along the column, because the partial pressure of CO_2 is practically equal to one in the upper part

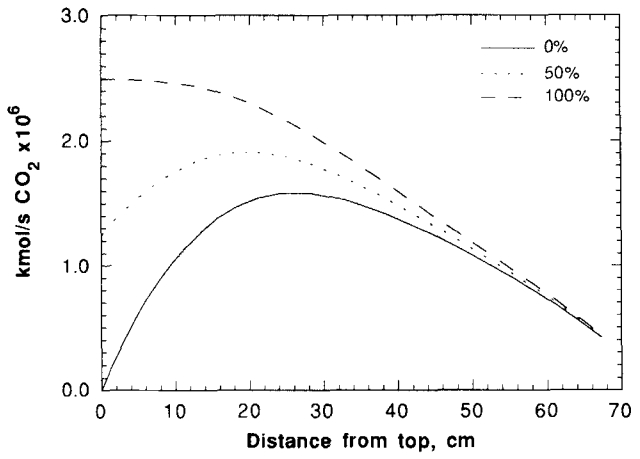

Figure 9. Computer results of dissolved CO_2 concentration along the column: 0, 50 and 100% saturation of the inlet cold water in CO_2.

of the column, and the CO_2 solubility in water decreases with increasing temperature.

It was initially thought that this experimental setup with the relatively high column may create particularly unfavorable conditions for the separation of the noncondensable gas from the condensate, since it would be required to drastically reduce at the bottom the high CO_2 concentrations reached at the top of the column. It turns out, however, that the CO_2 concentration of the outlet liquid stream is influenced mainly by the conditions at the lower end of the column, while the initial load of the incoming cold water has a minor effect. This conclusion, which is of vital importance in directing efforts of controlling the amount of gases dissolved, is amplified and supported by both the computational and the experimental results.

An indication, pointing to this kind of behavior, is found in the preliminary results of the numerical simulation. Shown in Figure 9 is the computed concentration of dissolved CO_2 along the column, plotted for three different saturation levels of the inlet water stream. It is evident that a wide variation of the inlet content has a minor effect on the amount of CO_2

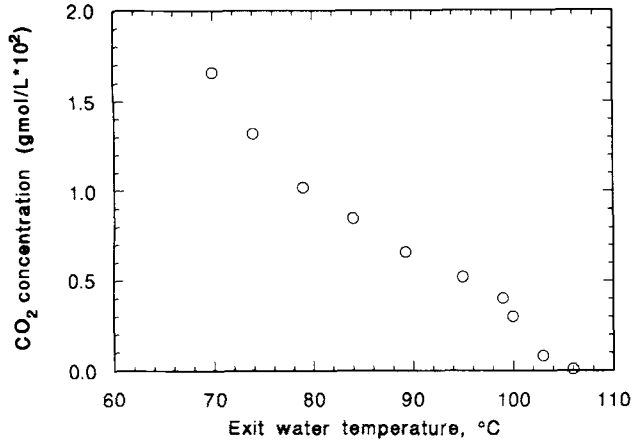

Figure 10. Measured CO_2 concentration in the effluent water as a function of exit temperature.

contained in the exit liquid. These results have only qualitative significance, since CO_2 absorption/desorption in the free space below the packing is not modeled.

The experimental data are measurements of dissolved gas concentration in the exit liquid, when a constant steam flow rate containing 3% w/w CO_2 is condensed by varying amounts of cold water. The data are correlated with the exit water temperature in Figure 10. Two points are worth discussing; the first is the trend in the variation of CO_2 concentration with water temperature, while the second is related to the actual values of measured concentration.

Figure 10 indicates that the percent gas absorbed is a strong function of the conditions at the bottom of the column. An increase of the water temperature by 30°C causes reduction of the CO_2 concentration in the liquid to 1/4 its original value. The total amount of CO_2 dissolved in the effluent liquid decreases even more drastically. This is so because higher water exit temperatures are followed by lower mass-flow rates, as is evident from an overall energy balance.

Granted that conditions at the bottom of the column determine the extent of gas absorption, the trend depicted in Figure 10 is in qualitative accord with the reverse effect of water temperature on gas solubility. However, the concentrations measured are much higher than the equilibrium values, predicted from Henry's law by using the mole fraction of CO_2 in the entrance steam. The difference between the two values amounts to 1-2 orders of magnitude for the lower exit liquid temperatures and decreases as the liquid temperature increases. This large discrepancy requires an explanation. It also needs to be mitigated in a full-scale system if the proposed method is to have any prospect as a gas separation technology. Indeed, calculations under realistic conditions (using saturated steam at 10 bar with 1% CO_2) indicate that the method is of potential interest only if the gas dissolved in the condensate is close to the equilibrium value predicted by Henry's law *on the basis of the bulk gas concentration at the bottom of the column.*

A tentative explanation put forward for the high gas absorption measured is the following: The rapid condensation of steam on the water film leads to CO_2 buildup at the vapor/liquid interface. As the condensation process is expected to be faster than gas absorption, it is this high instantaneous interfacial CO_2 concentration rather than the lower value in the bulk of the steam which provides the driving force for absorption. This proposed mechanism indicates a strong coupling between the processes of steam condensation and gas absorption that may have not been intuitively evident.

A limiting case, with maximum driving force, occurs when interfacial CO_2 concentrations are taken equal to the values calculated by neglecting gas solubility. This case corresponds to an absorption rate too small to affect the condensation process and can be implemented numerically in a simple way. Preliminary computational results using this assumption are in the order of magnitude that agrees with the experimental data. By contrast, calculations using the bulk gas concentration in the driving force give results 1-2 orders of magnitude lower than the data. Therefore, the preliminary numerical results seem to support the aforementioned tentative explanation.

For low exit water temperatures ($\epsilon_w < 1$), the bulk of condensation takes place at the bottom of the column and locally creates large interfacial concentrations of CO_2. Hence, the deviations from Henry's law, which appear more pronounced

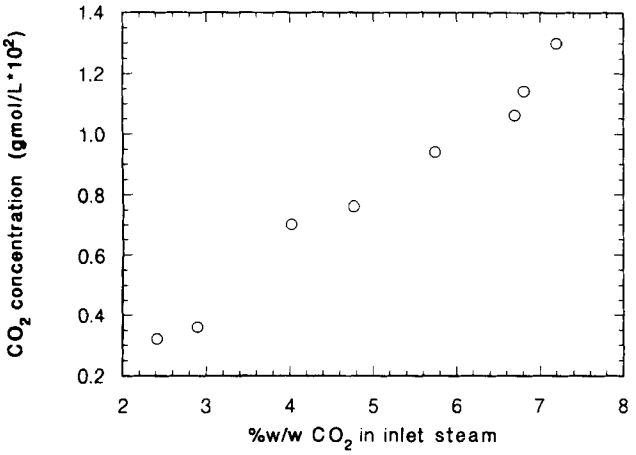

Figure 11. Measured CO_2 concentration of the effluent liquid as a function of the CO_2 content of inlet steam for water effectiveness $\epsilon_w \approx 1$.

for lower exit water temperatures (Figure 10), can be explained. This line of thought also suggests a way for minimizing CO_2 absorption. The optimum result corresponds to dissolved gas in equilibrium with the entrance steam and should, therefore, occur only if enough space is provided in the lower part of the column with the two fluids in thermal equilibrium. Such conditions under which no concentration gradient develops at the interface occur when $\epsilon_w \approx 1$ and correspond to a condensation zone rather far from the bottom of the column. A convincing example is provided by the last point in Figure 10, which corresponds to condensation starting 15–20 cm above the bottom of the packing. In this case, CO_2 concentration in the exit liquid is practically equal to the equilibrium prediction.

Finally, Figure 11 shows the results of a series of experiments with inlet steam containing varying amounts of CO_2, and water effectiveness $\epsilon_w \approx 1$. Inspection of the figure indicates that the concentration of CO_2 in the exit liquid scales roughly linearly with the CO_2 content of the steam.

Conclusions

A column filled with structured packing is tested as a direct-contact condenser of steam in counterflow with water, in the presence of noncondensables. Local heat-transfer coefficients are determined and shown to change along the column by roughly an order of magnitude. Overall performance is also expressed in terms of the height of a transfer unit, whose minimum value for the present configuration is approximately 5 cm.

A numerical simulation, based on the integration of local heat- and mass-transfer rates, offers predictions of heat-transfer coefficients in satisfactory agreement with the data. Thus, it is concluded that preliminary thermal designs of the present device can be obtained in a straightforward way using correlations from the literature. However, additional work is required to develop better correlations applicable to large amounts of noncondensables, and to address other relevant questions.

The amount of CO_2 retained in the water/condensate was measured for the special case when incoming cold water is saturated in CO_2 and was found to decrease with increasing water effectiveness, ϵ_w. For low temperature of the exit water ($\epsilon_w < 1$), the data are 1–2 orders of magnitude higher than predictions from Henry's law using the concentration of entrance steam, a discrepancy which diminishes with increasing condensate temperature. A tentative explanation is provided by considering a driving force for absorption based on the high interfacial CO_2 concentration developed because of condensation, rather than on the lower concentration in the bulk of the vapor phase.

There is presently an ongoing effort to improve the computational scheme by including the effect of the hot well and by providing versatility in the discretization of different regions of the column. The numerical results are expected to contribute to an improved understanding of the physical aspects of the problem and to a more realistic modeling of the rapidly changing conditions (flow rates, temperatures, concentrations) along the condenser. In particular, the approach seems highly appropriate for the complex problem of condensation coupled with partial dissolution of noncondensables in the liquid.

Acknowledgments

This work has been supported by the General Secretariat for Research and Technology of Greece and by the Commission of European Communities (under the programme VALOREN). The help of Dr. S. Paras and Mrs. K. Mouza in the preparation of the computerized data acquisition system is gratefully acknowledged.

Notation

C_p = specific heat
D = molecular diffusivity
h_g, h_l = partial heat-transfer coefficients in the vapor and liquid phase respectively
H_v = latent heat of vaporization of water
k_v, k_l = partial mass-transfer coefficients in the vapor and liquid phase respectively
N = molar flux of steam
p = partial pressure of steam
P = packing perimeter per unit column cross section
r = mass ratio of steam to water
Re = Reynolds number
Sh = Sherwood number
Sc = Schmidt number
u = fluid velocity
U_v = overall volumetric heat-transfer coefficient

Greek letters

Γ = liquid mass flow based on wetted perimeter
ϵ = void fraction of packing
θ = corrugation angle of packing
μ = liquid viscosity
ρ = density

Subscripts

b = bulk
eff = effective
g, v = vapor phase
i = interfacial
l = liquid phase
s = superficial
st = steam

Literature Cited

Awerbuch, L., V. Van der Mast, and M. Weckes, "Geothermal Flash Evaporation Process Technology," AIChE Meeting, Chicago (Nov., 1985).

Bharathan, D., and J. Althof, "An Experimental Study of Steam Condensation on Water in Countercurrent Flow in Presence of Inert Gas," *Proc. of ASME*, Paper 84-WA/Sol-25, New Orleans (1984).
Coury, G., "Geothermal Steam Purification by Evaporation to Improve Process Efficiency," AIChE Meeting, Chicago (Nov., 1985).
de Haan, A. B., and J. de Graauw, "Mass Transfer in Supercritical Extraction Columns with Structured Packing for Hydrocarbon Processing," *Ind. Eng. Chem. Res.*, **30**, 2463 (1991).
Fair, J. R., "Designing Direct-Contact Coolers/Condensers," *Chem. Eng.*, **2**, 91 (1972).
Fair, J. R., and J. L. Bravo, "Distillation Columns Containing Structured Packing," *Chem. Eng. Prog.*, **86**(1), 19 (1990).
Harriott, P., and H. Wiegandt, "Countercurrent Heat Exchange with Vaporizing Immiscible Transfer Agent," *AIChE J.*, **10**, 755 (1964).
Jacobs, H. R., K. D. Thomas, and R. F. Boehm, "Direct Contact Condensation of Immiscible Fluids in Packed Beds," *Condensation Heat Transfer*, ASME, New York, p. 103 (1979).
Jacobs, H. R., "Direct-Contact Condensation," *Direct-Contact Heat Transfer*, F. Kreith and R. F. Boehm, eds., Hemisphere, New York, p. 223 (1988).
Karapantsios, T. D., M. Kostoglou, and A. J. Karabelas, "Direct-Contact Condensation of Steam on Wavy Falling Films," *Meeting of Europ. Two-Phase Flow Group*, Stockholm (June, 1992).
Kreith, F., and R. F. Boehm, "Direct-Contact Heat Transfer Processes," *Direct-Contact Heat Transfer*, F. Kreith and R. F. Boehm, eds., Hemisphere, New York, p. 223 (1988).
Sideman, S., and D. Moalem-Maron, "Direct Contact Condensation," *Adv. Heat Transf.*, **15**, 227 (1982).
Sparrow, E. M., W. J. Minkowycz, and M. Saddy, "Forced Convection Condensation in the Presence of Noncondensables and Interfacial Resistance," *Int. J. Heat Mass Transf.*, **10**, 1829 (1967).
Treybal, R. E., *Mass-Transfer Operations*, McGraw-Hill, New York (1980).
Tung, V. X., and V. K. Dhir, "A Hydrodynamic Model for Two-Phase Flow through Porous Media," *Int. J. Multiphase Flow*, **14**, 47 (1988).
Wang, C.-Y., and C.-J. Tu, "Effects of Non-Condensable Gas on Laminar Film Condensation in a Vertical Tube," *Int. J. Heat Mass Transf.*, **31**(11), 2339 (1988).
Wilke, C. R., C. T. Cheng, V. L. Ledesma, and J. W. Porter, "Direct Contact Heat Transfer for Sea Water Evaporation," *Chem. Eng. Prog.*, **59**, 69 (1963).

Manuscript received July 6, 1993, and revision received Jan. 21, 1994.